IEEE Access
Multidisciplinary | Rapid Review | Open Access Journal

Received November 21, 2019, accepted December 9, 2019, date of publication December 16, 2019,
date of current version December 23, 2019.

Digital Object Identifier 10.1109/ACCESS.2019.2959941

Active Steering and Driving/Braking Coupled Control Based on Flatness Theory and A Novel Reference Calculation Method

YUQIONG WANG[1], SHUMING SHI[2], SONG GAO[1], YI XU[1], AND PENGWEI WANG[1]
[1]School of Transportation and Vehicle Engineering, Shandong University of Technology, Zibo 255049, China
[2]Transportation College, Jilin University, Changchun 130025, China

Corresponding author: Song Gao (gaosongsdut@163.com)

This work was supported in part by the Subproject of the National Key Research and Development Project of China under Grant 2016YFD0701101, in part by the National Natural Science Foundation of China under Grant 51905320, and in part by the Natural Science Foundation of Shandong Province under Grant ZR2018LF009.

ABSTRACT Vehicle handing stability under the combined acceleration steering and braking steering conditions has a great impact on the vehicle safety. Therefore, the coupled steering and driving/braking stability control is essential. Thus, a novel controller based on differential flatness and vehicle stability region is proposed. First, the reference vehicle state variables are calculated and the vehicle stability region is established based on vehicle dynamics and bifurcation analysis. Then, the flatness-based controller is designed which can ensure the vehicle handing stability by controlling the vehicle states approaching their references. Based on the driver preview model, the vehicle can keep good path tracking effect by tracking the lateral deviation. The simulation results of the double lane change tests show that the proposed control method can ensure both the vehicle handing stability and the path tracking effect. Compared to vehicle equipped with the integration of active front steering and direct yaw moment control, vehicle controlled by flatness-based controller performs better in both handing stability and path tracking.

INDEX TERMS Vehicle coupled control, differential flatness, stability region, handing stability, path tracking.

I. INTRODUCTION

The vehicle may lose its stability and cause heavy traffic accidents when running in high speed steering, acceleration steering or braking steering. It is necessary for the vehicle steering and driving/braking coupled control with the following coupling effects such as kinematic coupling and coupling of tire behavior. Thus, vehicle integrated control becomes the focus of the issue of vehicle handing stability control, and have been researched extensively.

The coordinated control of active front wheel steers (AFS) and direct yaw moment control (DYC) were firstly used for the vehicle integrated control [1]–[3]. Moreover, linear vehicle model and tire model was usually adopted for the controller design searched in the field of vehicle integrated control. However, the active steering angle and the stable yaw moment were taken as two independent control inputs, so the yaw moment generated by steering was neglected.

In order to take the neglected yaw moment into consideration and intensively study the optimum torque distribution to better control the vehicle, many researchers such as Abe [4], Hattori [5], Zhang [6] and Yu [7], [8] adopted hierarchical control structure for vehicle integrated control which firstly calculated the steering angle and reference yaw moment then distributed the braking torque to the four tires. However, the outcome will not be known yet if the total braking torques of the four wheels can not produce enough yaw moment restricted by the road adhesion. Thus it is necessary to slow down the vehicle in advance by driving control.

Few researchers took the driving torque into account for vehicle integrated control which can earlier actively control the longitudinal motion. Ono *et al.* [9], Fahimi [10], and Jiang *et al.* [11] studied the steering and driving/braking integrated control for four-wheel drive vehicle. L. Menhour and Fliess *et al* [12]–[14] utilized the flatness theory to

The associate editor coordinating the review of this manuscript and approving it for publication was Xiaosong Hu.

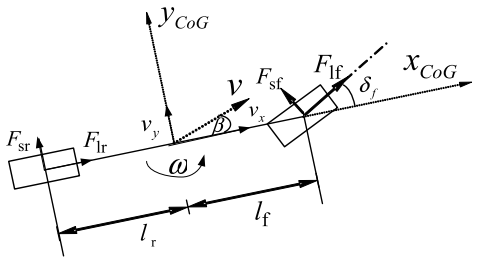

FIGURE 1. Single track vehicle model.

design the controller and achieved good path tracking effects. However, the longitudinal wind resistance was neglected, and the reference vehicle states used for the controller design were recorded with an instrumented vehicle by a professional driver in advance. For a common road that had not been driven by professional drivers, the expectation of controller would not be obtained. Thus, this reference acquisition method is not convenient for engineering application.

This paper proposes a coupled steering and driving/ breaking stability control method based on differential flatness theory and preview follower theory. The longitudinal wind resistance is considered in vehicle system modeling and the new reference calculation method based on road information and nonlinear dynamics bifurcation theory is proposed. The rest of this paper is organized as follows. The related models are presented in section II. Section III gives a detailed description about the calculation of reference vehicle variables. Section IV and section V give a detailed description about the design and verification of differential flatness-based integrated control algorithm. Section VI is the conclusion. The paper [15] is a first draft of this paper.

II. VEHICLE STEERING AND DRIVING/BREAKING MODEL

The planar motion stability is mainly considered than roll or pitch stability since the study is aimed at the coupled longitudinal and lateral control. The single track vehicle model with three degrees of freedom (longitudinal motion, lateral motion and yaw motion) depicted in figure 1 is considered in this paper in which oxy is the vehicle coordinate system. Air resistance plays an important role in longitudinal running resistance and is indispensable when vehicle runs in high speed. Different from paper [12]–[14], the influence of longitudinal wind resistance has been considered in this paper during vehicle system modeling. The three -degree-of-freedom (3DOF) vehicle dynamic model is established as (1).

$$\begin{cases} \dot{v}_x = v_y w + (F_{lf}\cos\delta - F_{sf}\sin\delta + F_{lr} - \rho C A v_x^2/2)/m \\ \dot{v}_y = -v_x\psi + (F_{lf}\sin\delta + F_{sf}\cos\delta + F_{sr})/m \\ \dot{w} = (F_{lf}l_f\sin\delta + F_{sf}l_f\cos\delta - F_{sr}l_r)/I_z \end{cases} \tag{1}$$

where m is the vehicle mass, I_z is the inertia moment about the vehicle vertical axis. v_x and v_y are the longitudinal and lateral velocities, respectively, w represents the vehicle yaw rate. δ is the steering angle of the front wheels. l_f and l_r are the distance from the vehicle gravity center to the front and rear axles, respectively, C is the longitudinal air resistance efficient, A represents the longitudinal windward area, ρ is the air density. F_{lf} and F_{lr} are the longitudinal force of front and rear wheels, respectively, F_{sf} and F_{sr} represent the lateral force of front and rear wheels, respectively.

The lateral and longitudinal forces of front and rear wheels can be calculated according to the vehicle dynamics model as follows:

$$\begin{cases} F_{sf} = C_f(\delta - \dfrac{v_y + wl_f}{v_x}) \\ F_{sr} = -C_f(\dfrac{v_y - wl_r}{v_x}) \end{cases} \tag{2}$$

$$\begin{cases} F_{lf} = (-I_w\dot{w}_f + T_t - T_{bf})/R_w \\ F_{lr} = (-I_w\dot{w}_r - T_{br})/R_w \end{cases} \tag{3}$$

where C_f and C_r represent the lateral stiffness of front and rear axles, respectively. T_t is the driving torque of front axle, T_{bf} and T_{br} are the braking torque of front and rear axles, respectively. I_w represents the wheel yaw moment of inertia, R_w represents the wheel rolling radius, ω_f and ω_r are the angular velocity of front and rear wheel, respectively.

Firstly, small steering angles are assumed as follows:

$$\cos\delta \approx 1, \quad \sin\delta \approx \delta \tag{4}$$

Then we take (2), (3) and (4) into (1), the differential equation of the three-degree-of-freedom dynamics model can be obtained as (5):

$$\begin{cases} m\dot{v}_x = mv_y w - \dfrac{I_w}{R_w}(\dot{w}_f + \dot{w}_r) + \dfrac{1}{R_w}(T_t - T_{bf} - T_{br}) \\ + C_f(\dfrac{v_y + wl_f}{v_x}) - C_f\delta^2 - \rho C A v_x^2/2 \\ m\dot{v}_y = -mv_x w - C_f(\dfrac{v_y + wl_f}{v_x}) - C_r(\dfrac{v_y - wl_f}{v_x}) \\ + \dfrac{1}{R_w}(T_t - T_{bf})\delta + (C_f - \dfrac{I_w}{R_w}\dot{w}_f)\delta \\ I_w\dot{w} = -l_f C_f(\dfrac{v_y + wl_f}{v_x}) + l_r C_r(\dfrac{v_y - wl_f}{v_x}) \\ + \dfrac{l_f}{R_w}(T_t - T_{bf})\delta + l_f(C_f - \dfrac{I_w}{R_w}\dot{w}_f)\delta \end{cases} \tag{5}$$

This dynamics model (5) introduces both steering angle of front wheel and the longitudinal driving torque and braking torque of the wheels. We can see that the longitudinal motion and lateral motion couple with each other obviously in (5). The longitudinal movement is controlled mainly via the driving/braking wheel torque and the lateral movement mainly via the steering angle δ. We denote the T_w as the subtraction of driving and braking torque of the axles which is expressed as:

$$T_w = T_t - T_b \tag{6}$$

where T_b represents the sum of T_{bf} and T_{br}. Then we denote the T_w and δ as two control variables expressed by:

$$\begin{cases} u_1 = T_w \\ u_2 = \delta \end{cases} \tag{7}$$

Then the system state space of the vehicle system model can be expressed as:

$$\dot{x} = g(x,t)u + h_1u_1u_2 + h_2u_2^2 + f(x,t) \tag{8}$$

where

$$x = \begin{bmatrix} v_x \\ v_y \\ w \end{bmatrix}, \quad u = \begin{bmatrix} u_1 \\ u_2 \end{bmatrix},$$

$$g(x,t) = \begin{bmatrix} 1/(mR_w) & C_f(v_y + wl_f)/(mv_x) \\ 0 & (C_fR_w - I_w\dot{w}_f)/(mR_w) \\ 0 & (l_fC_fR_w - l_fI_w\dot{w}_f)/(I_wR_w) \end{bmatrix},$$

$$h_1 = \begin{bmatrix} 0 \\ 1/(mR_w) \\ l_f/(I_wR_w) \end{bmatrix}, \quad h_2 = \begin{bmatrix} -C_f/m \\ 0 \\ 0 \end{bmatrix},$$

$$f(x,t) = \begin{bmatrix} v_yw - \frac{I_w}{mR_w}(\dot{w}_f + \dot{w}_r) - \frac{\rho CAv_x^2}{2m} \\ -v_xw - C_f(\frac{v_y + wl_f}{mv_x}) - C_r(\frac{v_y - wl_f}{mv_x}) \\ -l_fC_f(\frac{v_y + wl_f}{I_wv_x}) + l_rC_r(\frac{v_y - wl_f}{I_wv_x}) \end{bmatrix} \tag{9}$$

III. THE REFERENCE VEHICLE STATE VARIABLES

The control objectives should be defined before the controller design. There are two objectives: one is following the reference path exactly and the other one is keeping handing stability. The target path and the reference vehicle variables which can evaluate the vehicle handing stability should be studied firstly.

A. REFERENCE PATH

In recent years, we can obtain the road information with the fast development of computer vision. We assume that the road information is known in this paper. A double lane change path with sine function is applied which is usually used in the effect validation of steering and driving/braking coupled controller. The path has lateral skewing of 3.5 meters during longitudinal distance of 60 meters. The mathematical function of the path is expressed by (10):

$$y_{lat} = \begin{cases} 1.75\sin(\frac{x_l}{30}\pi - \frac{\pi}{2}) + 1.75 & (120 \le x_l \le 180) \\ 0 & (x_l < 120, x_l > 180) \end{cases} \tag{10}$$

where x_l represents the longitudinal location; y_{lat} is the lateral location.

B. REFERENCE LONGITUDINAL VELOCITY

Skilled drivers always decelerate when encountering a roundabout and then accelerate after driving out of the roundabout. It is essentially determined by the need for vehicle stability and can be seen from various simulation results in literature [14]. Due to vehicle longitudinal motion and lateral motion coupling with each other strongly, the longitudinal velocity in curve will smaller than that in straight road with the same driving torque. Thus we design the longitudinal velocity according to the rule of decelerating when encountering a roundabout and accelerating after driving out of the roundabout.

Set the entrance velocity, deceleration before roundabout, acceleration after roundabout, then the longitudinal velocity can be expressed as (11).

$$v_{ref} = \begin{cases} v_0 - a_1t & t_0 < t < t_1 \\ v_1 & t_1 < t < t_2 \\ v_1 + a_2t & t_2 < t < t_3 \end{cases} \tag{11}$$

where v_0 is the initial velocity, t_0 is the starting moment of decelerating, t_1 is the ending moment of decelerating and v_1 is the corresponding velocity in the moment of t_1, t_2 is the starting moment of accelerating, t_3 is the ending moment of accelerating.

Novices may slow down quickly to the absolute safety state and then make a turn when encounter a corner or obstacle; professional drivers may decelerate slightly and make a smooth turn; if both new and skilled drivers pay no attention to the corners or obstacles, they will lack enough time to decelerate. Therefore, we take the deceleration of -1.6m/s^2, -5m/s^2 and 0 into account to simulate the above three cases respectively.

C. REFERENCE YAW RATE

The vehicle stability control systems always make the vehicle actual states to track the reference state response through various control methods. In the study of vehicle stability control, reference yaw rate is widely used as the control target [17], which is a key parameter characterizing vehicle driving states and easy to be measured. Based on the linear two-degree-of-freedom model of the vehicle system dynamics, the reference yaw rate can be expressed by the relationship change with the front wheel angle [17], [19]. However the establishment of two-degree-of-freedom vehicle system dynamic model is based on the assumption of invariant longitudinal velocity.

In this paper, we will consider the effect of longitudinal velocity on vehicle handing stability. As the road information is known, the kinematic formula of steering in steady state is selected to calculate the reference yaw rate which reflects expectation of vehicle dynamic response of the drivers. It does not need to assume that the longitudinal velocity is a constant, and is not affected by vehicle mass, moment of inertia, tire cornering stiffness and other parameters. The reference yaw rate can be expressed by:

$$w_{ref} = \frac{v_{ref}}{R} \tag{12}$$

D. REFERENCE LATERAL VELOCITY

In the study of stability control for four-wheel steering vehicle, many papers such as [21] and [22] set the control reference of vehicle side-slip angle as zero and got many good control effects. The active steering angle of rear wheel can be controlled to the opposite direction of the front wheel. Thus it

is possible to keep the vehicle side-slip angle and the lateral velocity close to zero. However, the same control reference was used in the study of stability control for front-wheel steering vehicle [23]. The lateral velocity of the front wheel steering vehicle will not be zero without active steering rear wheel when vehicle turns a corner. It can be seen that the side-slip angle of the controlled vehicle was not controlled near zero, but varied with the change of the front wheel angle in the paper [23].

The rear wheels have no lateral velocity when the front wheel steering vehicle runs in a low speed and the vehicle lateral velocity is equal to the lateral velocity of the front wheel. Based on the linear vehicle model and linear tire model, the side-slip angel and the lateral velocity can be expressed by the relationship change with the front wheel angle which has been widely used in the vehicle stability control [17]. However, when the vehicle needs the stability controller to intervene, the general speed is relatively high. So in the study of vehicle stability control, low speed assumption is unreasonable and the linear model is undesirable.

Based on the nonlinear vehicle dynamics, Yang [24], Liu [25] studied the vehicle dynamic bifurcation characteristics affected by the vehicle inputs, and obtained equilibrium bifurcation results. They used the 3DOF vehicle model and got the similar conclusion: yaw rate and lateral velocity approximately proportional change with the front wheel angle in the stable region. But they neglected the tire longitudinal forces in vehicle model and did not describe the relationship between the lateral velocity and the yaw rate.

Based on the nonlinear 3DOF vehicle model and magic-formula tire model [26], by solving the equilibrium points under a certain speed, it is found that the lateral velocity and yaw rate are approximately proportional relation in the steady branch. The steady state is reference state in stability control, so the vehicle reference lateral velocity can be expressed by the equation:

$$w^{ref} = \lambda v_y^{ref} \tag{13}$$

The relationship that the equilibrium points vary with the front wheel angle is affected by different longitudinal velocities and tire-road adhesion coefficients. The estimation of vehicle dynamics states such as velocity, side-slip angle and road-tire friction coefficient is important and has been researched extensively [16]–[18]. However, vehicle dynamics states estimation is not the main theme of this paper. We estimate the lateral velocity according to the preliminary study [34] of our research group. The high adhesion road is researched in this paper, so it is necessary to require the proportion of stable yaw rate and lateral velocity in different vehicle speed. Simulation research in this paper used the following parameters: $m = 1515\text{kg}$, $I_z = 1680\text{kg.m}^2$, $l_f = 1.209$, $l_r = 1.533$.

We firstly solve the stable equilibrium points when the vehicle initial speed is 25m/s using genetic algorithm. Then we can obtain the proportional coefficient λ making use of MATLAB's cftool toolbox as shown in figure 2. Then we

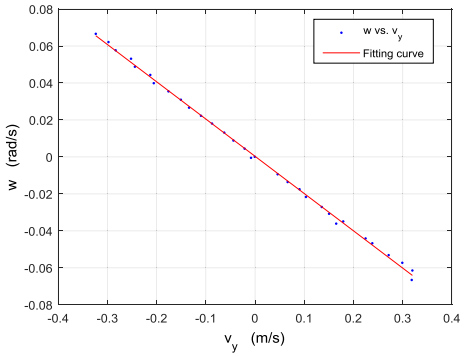

FIGURE 2. The v_y-w value of partial stable equilibrium points($v_0 = 25$m/s).

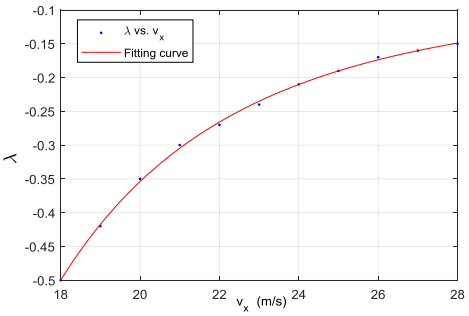

FIGURE 3. Relationship between longitudinal velocity and proportional coefficient in steady equilibrium state.

TABLE 1. The proportion of stable yaw rate and lateral velocity in different vehicle speeds.

v_x(m/s)	λ	v_x(m/s)	λ
18	-0.50	24	-0.21
19	-0.42	25	-0.19
20	-0.35	26	-0.17
21	-0.3	27	-0.16
22	-0.27	28	-0.15
23	-0.24		

calculated the λ in various speeds shown in Table 1 on the high adhesion coefficient road and thus fitted the values as shown in figure 3. The fitting curve can be expressed by:

$$\lambda = -55630 v_x^{-4.039} - 0.07462 \tag{14}$$

By combining (12),(13) and (14), we can get the expression of the reference lateral velocity as shown in (15).

$$v_y^{ref} = \frac{v_x^{ref}/R}{-55630(v_x^{ref})^{-4.039} - 0.07462} \tag{15}$$

IV. STEERING AND DRIVING/BRAKING COUPLED CONTROLLER DESIGN

The subsystems of coordinated control and hierarchical control have their own control algorithms, such as PID control [27], intimal model control [28], optimal control [29], sliding mode control [30] and model predictive control [31], etc. PID control does not need to know the precise mathematical

model of the controlled object and can achieve satisfactory results which is widely used in engineering application, but it does not suitable for the complicated nonlinear system. Different from classical control algorithms such as PID, modern control algorithms and intelligent control algorithms are both suitable for linear system and nonlinear time-varying system, but have some disadvantages: the optimal control is not suitable for the case where the parameters of the controlled object are unknown or vary greatly, and the system at this time is no longer optimal and even unstable; sliding mode control needs to overcome the chattering phenomenon; model predictive control needs to ensure the stability of the algorithm and is difficult in numerical solution. Thus we consider to linearize the vehicle system and then we can use classical control algorithm for the coupled control.

According to the flatness theory proposed by Fliess *et al.* [32], if a flat output could be found, the system would be linearization system and could be controlled using linear control method. So the flatness-based control method is considered for the vehicle in this paper.

The definition of differential flat system is defined as the following [32]:

$$\dot{x} = f(x, u), x \in R^n, \quad u \in R^m \tag{16}$$

$$y = F(x, u, \dot{u}, \cdots u^{(i)}), \quad y \in R^m \tag{17}$$

$$\begin{cases} x = \zeta_x(y, \dot{y}, \cdots y^{(i)}) \\ u = \zeta_u(y, \dot{y}, \cdots y^{(i)}) \end{cases} \tag{18}$$

Considering a nonlinear system expressed by (16), where x is the state variable, u is the input of system. If the output form like (17) exits, the system state x and input u may be written in the form like (18), then the system is differential flat and y is the differential flat output.

For vehicle system, we first assume that the vehicle system (8) is a differential flat system and try to select a group of outputs. According to the properties of flat system, the number of flat outputs is the same as the number of system inputs. As shown in (7), there are two inputs (T_w and δ) in the vehicle system, so the number of vehicle system flat outputs is also two. Since the flat output is represented by the state and its finite order derivative as (17) shows, we first consider to express the two outputs using the three states (longitudinal velocity, lateral velocity and yaw rate). The longitudinal velocity is affected by the driving or braking torque T_w, the lateral velocity and yaw rate by the steering angle δ to a large extent. Therefore, the longitudinal velocity is considered as one of the outputs, and the linear combination of lateral velocity and yaw rate is considered as another. According to coefficient observation of the second and third formulas in (5), we try to neglect the higher-order terms and set the two flat outputs as:

$$\begin{cases} y_1 = v_x \\ y_2 = l_f m v_y - I_z w \end{cases} \tag{19}$$

Taking a derivative of the second flat output, we can obtain:

$$\dot{y}_2 = l_f m \dot{v}_y - I_z \dot{w} = -l_f m w v_x - l C_r \frac{v_y - w l_2}{v_x} \tag{20}$$

Substituting (19) and (20) into (17), we can deduce the expression of vehicle states about the flat outputs:

$$\begin{bmatrix} v_x \\ v_y \\ w \end{bmatrix} = \begin{bmatrix} y_1 \\ \frac{y_2}{l_f m} - \frac{I_z(l_f m y_1 \dot{y}_2 + C_r l y_2)}{l_f m(l C_r(I_z - l_f l_r m) + l_f^2 m^2 y_1^2)} \\ -\frac{l_1 m y_1 \dot{y}_2 + C_r l y_2}{l C_r(I_z - l_f l_r m) + l_f^2 m^2 y_1^2} \end{bmatrix} \tag{21}$$

Since the vehicle control inputs T_w and δ are not shown in (19) and (20), we further calculate the derivative of y_1 and we can obtain:

$$\dot{y}_1 = \frac{1}{mR} T_w + \frac{C_f}{m}\left(\frac{v_y + w l_f}{v_x}\right)\delta + w v_y - \frac{I_w}{mR}(\dot{w}_r + \dot{w}_f) - \frac{\rho}{2m} C_x A_x v_x^2 \tag{22}$$

The equation (22) can be expressed as follow:

$$\dot{y}_1 = \Delta_{11} T_w + \Delta_{12}\delta + F_1 \tag{23}$$

where

$$\Delta_{11} = \frac{1}{mR}$$

$$\Delta_{12} = \frac{C_f}{m}\left(\frac{v_y + w l_f}{v_x}\right)$$

$$F_1 = w v_y - \frac{I_w}{m R_w}(\dot{w}_r + \dot{w}_f) - \frac{\rho}{2m} C A v_x^2$$

Similarly, by taking a derivative of $\dot{y}_2$, we can obtain:

$$\ddot{y}_2 = \frac{l C_r v_y - l_r l C_r w - l_f m w v_x^2}{v_x^2}\dot{v}_x + \frac{l_r l C_r - l_f m v_x^2}{v_x}\dot{w} - \frac{l C_r}{v_x}\dot{v}_y \tag{24}$$

By substituting the vehicle model (8) into (24) and neglect the high-order terms of T_w and δ as $h_1 u_1 u_2$ and $h_2 u_2^2$, we can get the relationship between $\ddot{y}_2$ and $T_w\delta$ as shown in (25). The influence analysis simulation of neglecting the high-order terms will be introduced in Section V.

$$\ddot{y}_2 = \Delta_{21} T_w + \Delta_{22}\delta + F_2 \tag{25}$$

where

$$\Delta_{21} = \frac{C_r l(v_y - w l_r) - l_f m w v_x^2}{m R_e v_x^2}$$

$$\Delta_{22} = \frac{(l_r C_r l - l_f m v_x^2) l_f (C_f R_e - I_w \dot{w}_f)}{v_x I_z R_e} - \frac{C_r l(C_f R_e - I_w \dot{w}_f)}{m R_e v_x} \cdots + \frac{(C_r l(v_y - w l_2) - l_1 m w v_x^2) C_f (v_y + w l_1)}{m v_x^3}$$

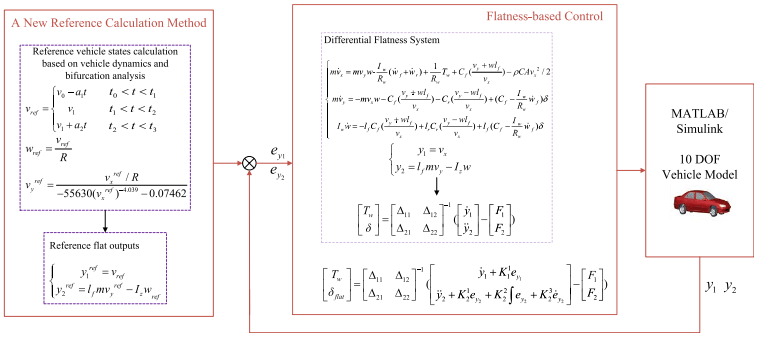

FIGURE 4. The flatness-based controller.

$$F_2 = \frac{(C_r l(v_y - wl_2) - l_f m w v_x^2)}{v_x^2} f_1 - \frac{C_r l}{v_x} f_2 + \frac{(C_r l_2 l - l_f m v_x^2)}{v_x} f_3$$

$$f_1 = w v_y - \frac{I_w(\dot{w}_f + \dot{w}_r)}{m R_e}$$

$$f_2 = -w v_x - \frac{C_f(v_y + w l_f) + C_r(v_y - w l_r)}{m v_x}$$

$$f_3 = \frac{-l_f C_f(v_y + w l_f) + l_2 C_r(v_y - w l_r)}{v_x}$$

In order to solve the vehicle control inputs T_w and δ, we combine (23) and (25) to simultaneous equations:

$$\begin{bmatrix} \dot{y}_1 \\ \ddot{y}_2 \end{bmatrix} = \begin{bmatrix} \Delta_{11} & \Delta_{12} \\ \Delta_{21} & \Delta_{22} \end{bmatrix} \begin{bmatrix} T_w \\ \delta \end{bmatrix} + \begin{bmatrix} F_1 \\ F_2 \end{bmatrix} \tag{26}$$

To solve the determinant of coefficient matrix, (27) can be obtained:

$$\begin{vmatrix} \Delta_{11} & \Delta_{12} \\ \Delta_{21} & \Delta_{22} \end{vmatrix} = \Delta_{11}\Delta_{22} - \Delta_{12}\Delta_{21} = \frac{(I_w \dot{w}_f - C_f R_e)(l_f^2 v_x^2 m^2 - C_r l_f l_r l m + C_r I_z l)}{I_z R_e^2 m^2 v_x} \tag{27}$$

Because

$$I_w \dot{w}_f \ll C_f R_e$$
$$I_z \neq m l_f l_r$$

Therefore

$$(I_w \dot{w}_f - C_f R_e)(l_f^2 v_x^2 m^2 - C_r l_f l_r l m + C_r I_z l) \neq 0$$

In addition

$$I_z R_e^2 m^2 v_x > 0$$

There is

$$\begin{vmatrix} \Delta_{11} & \Delta_{12} \\ \Delta_{21} & \Delta_{22} \end{vmatrix} \neq 0$$

By solving the simultaneous equations (26) in reverse, we can obtain the expression of control inputs about the flat outputs and their derivatives:

$$\begin{bmatrix} T_w \\ \delta \end{bmatrix} = \begin{bmatrix} \Delta_{11} & \Delta_{12} \\ \Delta_{21} & \Delta_{22} \end{bmatrix}^{-1} \left(\begin{bmatrix} \dot{y}_1 \\ \ddot{y}_2 \end{bmatrix} - \begin{bmatrix} F_1 \\ F_2 \end{bmatrix} \right) \tag{28}$$

In this way, both the system state x and input u would be expressed by the flat output. On the other hand, the vehicle system is a differential flat system.

The flatness-based handing stability controller is designed which made it possible to obtain the reference vehicle inputs through the vehicle outputs and their errors:

$$\begin{bmatrix} T_w \\ \delta_{flat} \end{bmatrix} = \begin{bmatrix} \Delta_{11} & \Delta_{12} \\ \Delta_{21} & \Delta_{22} \end{bmatrix}^{-1} \times \left(\begin{bmatrix} \dot{y}_1 + K_1^1 e_{y_1} \\ \ddot{y}_2 + K_2^1 e_{y_2} + K_2^2 \int e_{y_2} + K_2^3 \dot{e}_{y_2} \end{bmatrix} - \begin{bmatrix} F_1 \\ F_2 \end{bmatrix} \right) \tag{29}$$

where

$$e_{y1} = y_1^{ref} - y_1 = v_x^{ref} - v_x,$$
$$e_{y2} = y_2^{ref} - y_2 = l_f m(v_y^{ref} - v_y) - I_z(w^{ref} - w)$$

K_1^1 K_2^1 K_2^2 and K_2^3 are the coefficient of the error and the control parameters that need to be designed. The flatness-based controller frame is shown in figure 4.

In order to help keeping vehicle path tracking along with vehicle handing stability, the optimal preview curvature model was established which could calculate the front wheel steering angle by calculating the trajectory deviation shown as (30). The model is mildly nonlinear by relaxing the constant v_x assumption. It provides an effective and direct method for describing the driver's desired behavior characteristics. At the same time, the model has clear physical concept, simple operation structure and is convenient for engineering application [33].

$$\delta_{driver} = \frac{2L}{d^2} [f(t+T) - y(t) - T \times \dot{y}] \tag{30}$$

where δ_{driver} is the steering angle of front wheels, $y(t)$ represent the lateral position of the car, d is the looking forward distance, $\dot{y}(t)$ and $\dot{x}(t)$ represent the lateral and longitudinal velocity of the vehicle on the absolute inertial coordinate; T is the looking forward time which can be expressed as $T = d/\dot{x}(t)$.

Based on the flatness theory and PID controller, we can obtain the reference vehicle inputs T_w and δ_{flat} which can ensure the handing stability by controlling the vehicle states approaching their references. Based on the driver preview

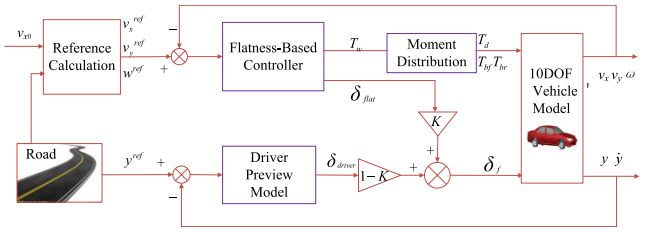

FIGURE 5. The diagram of the integrated control system.

model, the vehicle can keep good path tracking effect by tracking the lateral deviation. Both the driver preview model and the flatness-based controller exported a steering angle, so the final steering wheel angle weighted by the two angles is considered to control the vehicle as shown in (31), in this way the vehicle can both keep its stability and make a good path tracking. The diagram of the integrated control system is shown in figure 5.

$$\delta_f = K\delta_{flat} + (1-K)\delta_{driver}, \quad 0 < K < 1 \tag{31}$$

For the distribution of driving/ braking torque: $T_w > 0$ as the driving moment, the left and right wheels have the same value. $T_w < 0$ as the braking torque, the front and back wheels torque are distributed as: $T_{bf} = 1.85\, T_{br}$ [20].

V. SIMULATION RESULTS AND ANALYSIS

The Vehicle Organization Simulation System (VOSS) based on MATLAB/Simulink [34] is used for the simulation. This simulation model includes the road model, the driver preview model and the ten degree of freedom vehicle model. The tire model uses the tire mixed slip magic formula model under high adhesion road as the literature [26].

The controller parameters are calibrated using the parameters of a certain car, then $K_1^1 = 1$, $K_2^1 = 60$, $K_2^2 = 12$, $K_2^3 = 0$, and $K = 0.4$ are obtained. The simulation and analysis of the open-loop test and close-loop test are shown in the rest of this Section.

A. OPEN-LOOP TEST

In order to analyze the effectiveness of the proposed integrated control system under the open-loop experiment, a cycle sinusoidal of 30deg/0.25Hz steering wheel angel input is given, the vehicle speed is set at 30m/s and the and the tire–road adhesion coefficient is set to 0.85. This steering input approximately represents an emergency single lane change maneuver. The simulation results are shown in figure 5. The figure 6 (a) express that the vehicle equipped with the coupled controller can complete the emergency single lane change maneuver smoothly. As shown in figure 6 (b), the coupled control system can track the reference yaw rate during the cycle maneuver, but the yaw rate response of uncontrolled vehicle changed dramatically and return to zero on straight line much later than the controlled system. The same condition also occurred in the side-slip angle response as shown in figure 6 (c), the phase plan envelope of β-β' with controller on is smaller than that without the controller.

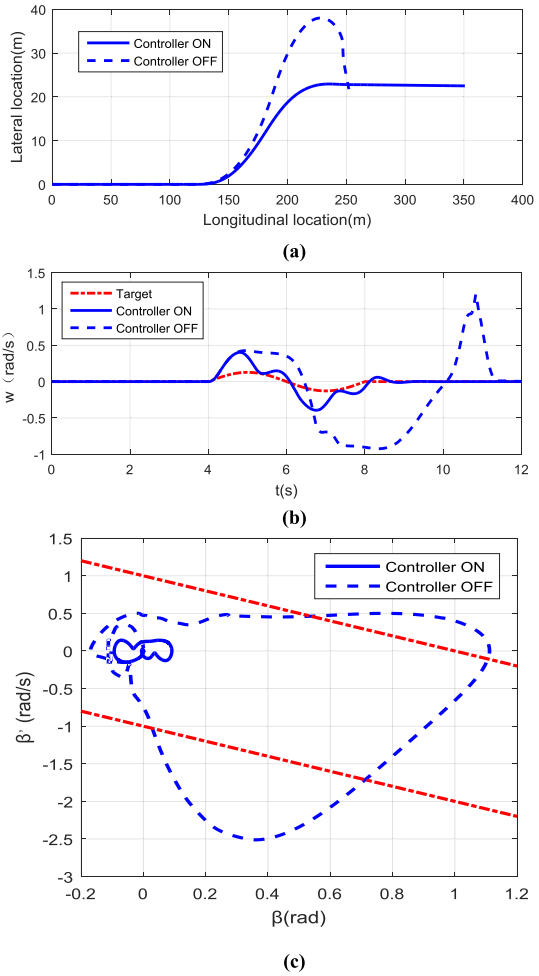

FIGURE 6. The effects of flatness-based control, (a) vehicle trajectory, (b) yaw rate response, (c) phase plan of β-β'.

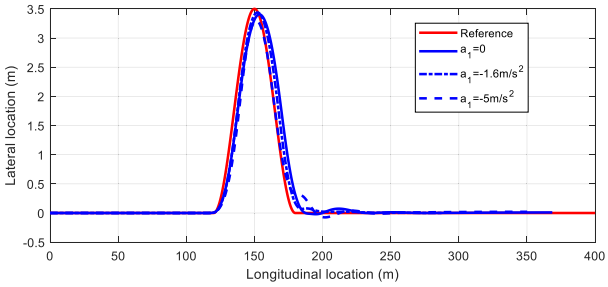

FIGURE 7. The path tracking effect in different reference longitudinal velocity.

B. CLOSED-LOOP TEST

According to driving experiences, novice drivers may slow the vehicle down quickly to the absolute safety state and then make a turn when encounter a corner or obstacle; experienced drivers may decelerate slightly and make a smooth turn; if both novice and experienced drivers pay no attention to the corners or obstacles, or they are too close to the obstacles, they will lack enough time to decelerate.

In order to verify the robustness of the steering and driving/braking coupled controller in different driving conditions, we take the deceleration of -1.6m/s^2, -5m/s^2 and 0m/s^2

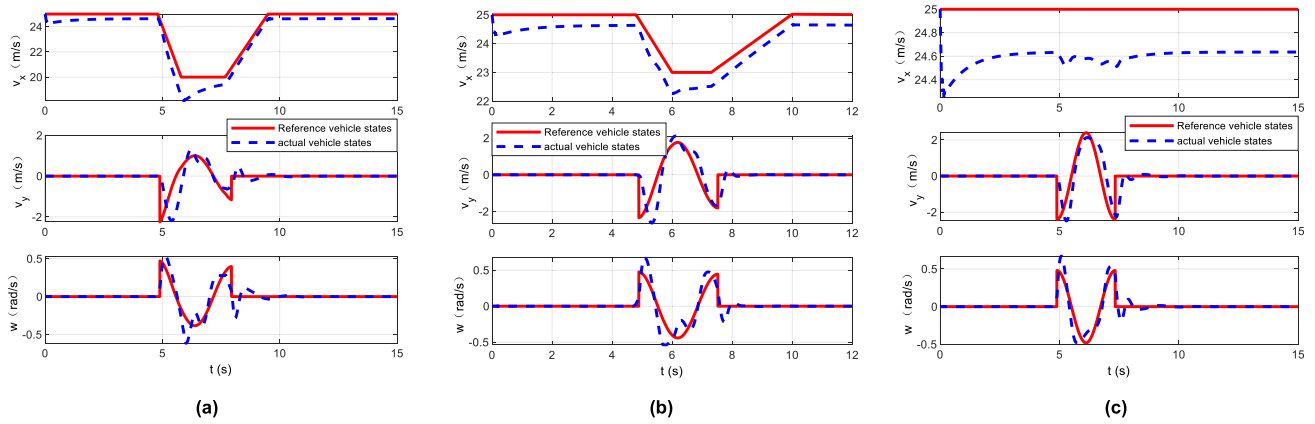

FIGURE 8. The vehicle variables response with their reference, (a) novel driver response ($a_1 = -5\text{m/s}^2$), (b) experienced driver response ($a_1 = -1.6\text{m/s}^2$), (c) response in unexpected situation($a_1 = 0\text{m/s}^2$).

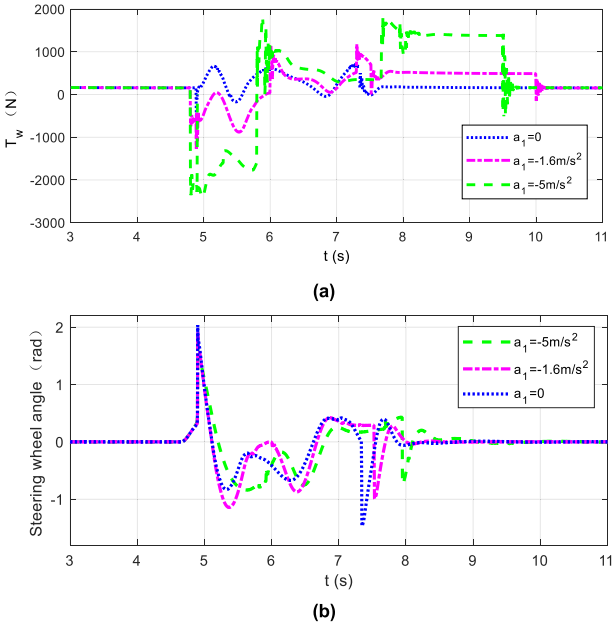

FIGURE 9. The outputs of the coupled steering and driving/braking controller in different driving conditions, (a) driving/braking torque, (b) steering wheel angle.

into account to simulate the above three cases respectively. Figure 7-9 show the path tracking effects, vehicle output variables, and vehicle control inputs in different longitudinal velocity planning respectively.

As shown in figure 7 that the vehicle has a relatively good path tracking performance. The trajectory has small lateral deviation: the error is not more than 0.15 meters when the deceleration is zero; the error is not more than 0.12 meters when the deceleration is -1.6 m/s^2; the error is not more than 0.35 meters when the deceleration is -5 m/s^2.

Figure 8 shows that the vehicle longitudinal velocity, lateral velocity and the yaw rate can track their references smoothly in the cases whether the vehicle is driven by a novice ($a_1 = -5\text{m/s}^2$) or experienced person ($a_1 = -1.6\text{m/s}^2$), or in unexpected situation($a_1 = 0\text{m/s}^2$).

As shown in figure 9 (a), the driving torque remains at around 160Nm when the vehicle goes straight at a constant speed and will change with the curve when vehicle makes a turn. The smaller the deceleration is, the smaller the driving torque or braking torque is. Transmission ratio of steering system between the steering wheel angle and front wheel angle is set as 20. The steering wheel angle of the controller output as well as the vehicle input is shown in figure 9 (b). The larger the deceleration is, the longer the steering time is. The steering wheel angle changes quickly at the start moment and end moment of the corner. It is caused by the suddenly changing curvature of the reference trajectory expressed by equation (10), and it also shows that the controller can track the desired trajectory quickly and accurately at the same time. In the future, we will optimize the reference trajectory to make the vehicle control input smoother.

It is shown in figure 7-9 that the vehicle can keep both path tracking and handing stability very well by the steering and driving /braking coupled control and the controller is robust in different driving conditions.

The simulation of the vehicle with different controllers has been compared to further evaluate the control benefits. The longitudinal speed is set at 100km/h. Figure 10 (a) shows that the coupled control vehicle shows smaller lateral deviation than vehicle equipped with DYC or AFS+DYC. As shown in figure 10 (b), the vehicle equipped with DYC or AFS+DYC shows larger fluctuation range of vehicle side-slip angle and its change rate than the coupled control vehicle. We can see in figure 10 that the coupled control vehicle has better path tracking effects and handing stability than the vehicle controlled by single DYC or combined AFS with DYC.

C. CONTROLLER DESIGN ERROR SIMULATION

We have neglected the high-order terms of T_w and δ ($h_1u_1u_2$ and $h_2u_2^2$) to express the relationship between the flat output and T_w δ as shown in (25). We can see in equation (8) that $h_1u_1u_2$ mainly affect the second and third formula i.e. the value of lateral acceleration and yaw rate, $h_2u_2^2$ mainly affect

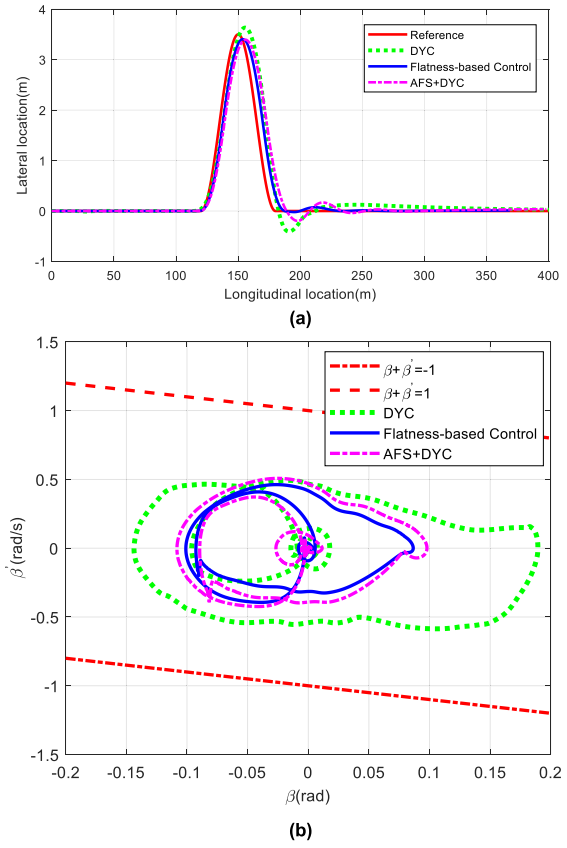

FIGURE 10. The simulation results in different control modes, (a) the path tracking effect, (b) the phase plane of β-β'.

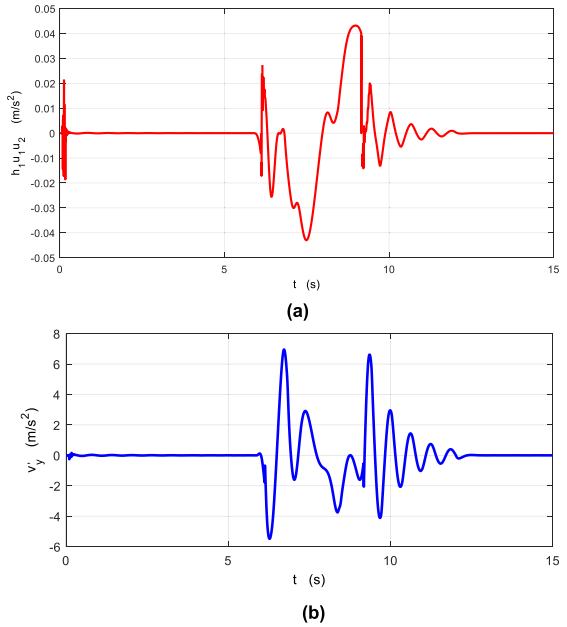

FIGURE 11. The simulation comparison of neglected high-order term $h_1u_1u_2$, (a) the value of $h_1u_1u_2$, (b) the value of lateral acceleration.

the first formula i.e. the value of longitudinal acceleration. The simulation comparison of the elimination term and the total value of the formula are given in figure 11 as an example to verify the feasibility of eliminating the item $h_1u_1u_2$ of equation (8) in the controller design process. It can be seen that the value of the elimination term $h_1u_1u_2$ is about 100 times smaller than the overall value and is not enough to affect the lateral acceleration. Using the same comparison method, we can verify the feasibility of eliminating the item $h_2u_2^2$. Thus the performance of the control law is not affected by the model simplifications.

VI. CONCLUSION

This paper proposes a flatness-based steering and driving/braking coupled control strategy for vehicles. Aimed at the strong nonlinear and dynamic coupling effects between the lateral and longitudinal motion, the lateral and longitudinal coupling vehicle models were established. The longitudinal tire forces and air resistance were introduced in the vehicle modeling of controller design preciously. Then, a novel vehicle stability region with variable longitudinal velocity was proposed based on road information and nonlinear dynamic bifurcation theory. The reference vehicle states used for the controller design can be solved offline and need not to be driven by professional drivers in advance. Thus, this reference acquisition method is convenient for engineering application.

The flatness-based controller can ensure the vehicle handing stability by controlling the vehicle states approaching their reference stable states. Combined with driver preview model, the vehicle can keep good path tracking effect simultaneously by tracking the lateral deviation. The simulation results of the emergency double lane change tests show that the proposed control strategy performs better in both handing stability and path tracking than integrated AFS and DYC.

However, the real vehicle test was not carried due to potential danger. Future work will focus on the simulation of low friction surfaces and hardware-in-the-loop simulations.

REFERENCES

[1] M. Selby, W. J. Manning, and M. D. Brown, "A coordination approach for DYC and active front steering," in *Proc. SAE World Congr.*, Mar. 2001.

[2] M. Nagai, M. Shino, and F. Gao, "Study on integrated control of active front steer angle and direct yaw moment," *JSAE Rev.*, vol. 23, no. 3, pp. 309–315, 2002.

[3] A. Goodarzi and M. Alirezaie, "A new fuzzy optimal integrated AFS/DYC control strategy," presented at the AEC, 2006.

[4] O. Mokhiamar and M. Abe, "Simultaneous optimal distribution of lateral and longitudinal tire forces for the model following control," *J. Dyn. Syst., Meas., Control.*, vol. 126, pp. 753–763, Dec. 2004.

[5] Y. Hattori, K. Koibuchi, and T. Yokoyama, "Force and moment control with nonlinear optimum distribution for vehicle dynamics," presented at the AVEC, Hiroshima, Japan, 2002.

[6] R.-H. Zhang, Z.-C. He, H.-W. Wang, F. You, and K.-N. Li, "Study on self-tuning tyre friction control for developing main-servo loop integrated chassis control system," *IEEE Access*, vol. 5, pp. 6649–6660, 2017.

[7] D. F. Li, S. Q. Du, and F. Yu, "Integrated vehicle chassis control based on direct yaw moment, active steering and active stabilizer," *Vehicle Syst. Dyn.*, vol. 46, no. S1, pp. 341–351, 2008.

[8] X. Shen and F. Yu, "Study on vehicle chassis control integration based on a main-loop-inner-loop design approach," *Automobile Eng.*, vol. 220, no. 11, pp. 1491–1502,2006.

[9] E. Ono, Y. Hattori, Y. Muragishi, and K. Koibuchi, "Vehicle dynamics integrated control for four-wheel-distributed steering and four-wheel-distributed traction/braking systems," *Vehicle Syst. Dyn., Int. J. Vehicle Mech. Mobility*, vol. 44, no. 2, pp. 139–151, 2006.

[10] F. Fahimi, "Full drive-by-wire dynamic control for four-wheel- steer all-wheel-drive vehicles," *Vehicle Syst. Dyn.*, vol. 51, no. 3, pp. 360–376, 2013.
[11] L. Jiang, H. Qiu, J. Yang, S. Huang, L. Ma, and S. Qiu, "Coordinated control strategy of EPS and TCS for four-wheel drive vehicle," in *Proc. 9th Int. Symp. Comput. Intell. Design (ISCID)*, Dec. 2016, pp. 148–153.
[12] L. Menhour, B. d'Andréa-Novel, C. Boussard, M. Fliess, and H. Mounier, "Algebraic nonlinear estimation and flatness-based lateral/longitudinal control for automotive vehicles," in *Proc. IEEE Int. Conf. Intell. Transp. Syst.*, Oct. 2011, pp. 463–468.
[13] L. Menhour, B. d'Andréa-Novel, M. Fliess, and H. Mounier, "Multivariable decoupled longitudinal and lateral vehicle control: A model-free design," in *Proc. 52nd IEEE Conf. Decision Control (CDC)*, Dec. 2013, pp. 2834–2839.
[14] L. Menhour, B. d'Andréa-Novel, M. Fliess, and H. Mounier, "Coupled nonlinear vehicle control: Flatness-based setting with algebraic estimation techniques," *Control Eng. Pract.*, vol. 22, no. 1, pp. 135–146, 2014.
[15] Y. Q. Wang, S. M. Shi, and L. Li, "Flatness-based vehicle coupled control for steering stability and path tracking," in *Proc. SAE-China Conf.*, Shanghai, China, Dec. 2015, pp. 49–60.
[16] S. M. Shi, L. Henk, and B. Paul, "Estimation of vehicle side slip angle based on fuzzy logic," *Vehicle Eng.*, vol. 27, no. 4, pp. 426–430, 2005.
[17] L. Li, "Progress on vehicle dynamics stability control system," *Jixie Gongcheng Xuebao*, vol. 49, no. 24, pp. 95–107, 2013.
[18] S. Cheng, M. Mei, and X. Ran, "Adaptive unified monitoring system design for tire-road information," *ASME. J. Dyn. Sys., Meas., Control*, vol. 141, no. 7, pp. 1–11, 2019.
[19] J. Wu, S. Cheng, and B. Liu, "A human-machine-cooperative-driving controller based on AFS and DYC for vehicle dynamic stability," *Energies*, vol. 10, no. 11, pp. 1–18, 2017.
[20] Z. S. Yu, "Vehicle braking performance," in *Automobile Theory*, 5th ed. Beijing, China: China Machine Press, 2007, ch. 4, sec. 5, pp. 116–118.
[21] J. Men, B. Wu, and C. Jie, "Comparisons of vehicle stability controls based on 4WS, brake, brake-FAS and IMC techniques," *Vehicle Syst. Dyn.*, vol. 50, no. 7, pp. 1053–1084, 2012.
[22] M. Li and Y. Jia, "Decoupling control in velocity-varying four-wheel steering vehicles with H_∞ performance by longitudinal velocity and yaw rate feedback," *Vehicle Syst. Dyn.*, vol. 52, no. 12, pp. 1563–1583, 2014.
[23] B. L. Boada, M. J. L. Boada, and V. Díaz, "Fuzzy-logic applied to yaw moment control for vehicle stability," *Vehicle Syst. Dyn.*, vol. 43, no. 10, pp. 753–770, 2005.
[24] X. J. Yang, "Research on the nonlinear dynamics and active control for vehicle cornering destabilization in critical situations," Ph.D. dissertation, School Mech. Eng., Shandong Univ., Jinan, China, 2009.
[25] L. Liu, "Nonlinear analysis and control strategy evaluation on the stability of vehicle 3-DOF planar motion," Ph.D. dissertation, School Transp., Jilin Univ., Changchun, China, 2010.
[26] S. M. Shi, L. Li, and X. B. Wang, "Analysis of the vehicle driving stability region based on the bifurcation of the driving torque and the steering angle," *Proc. Inst. Mech. Eng. D, J. Automobile Eng.*, vol. 231, no. 7, pp. 984–988, 2017.
[27] X. J. Gao, Z. P. Yu, and Z. L. Amp, "The principle and application of mechanical active front steering system," *Automobile Eng.*, vol. 28, no. 10, pp. 913–918, 2006.
[28] J. Wu, Y. Q. Zhao, and X. W. Ji, "A modified structure internal model robust control method for the integration of active front steering and direct yaw moment control," *Sci. China. Technol. Sc.*, vol. 58, no. 1, pp. 75–85, 2015.
[29] D. L. Chen, C. L. Yin, and L. Chen, "Study on active front steering based on state-space observer," *Zhongguo Jixie Gongcheng*, vol. 18, no. 24, pp. 3019–3023, Dec. 2007.
[30] P. W. Wang, S. Gao, L. Li, S. Cheng, and L. Zhao, "Automatic steering control strategy for unmanned vehicles based on robust backstepping sliding mode control theory," *IEEE Access*, vol. 7, pp. 64984–64992, 2019.
[31] S. Cheng, L. Li, M.-M. Mei, Y.-L. Nie, and L. Zhao, "Multiple-objective adaptive cruise control system integrated with DYC," *IEEE Trans. Veh. Technol.*, vol. 68, no. 5, pp. 4550–4559, May 2019.
[32] M. Fliess, J. Lévine, P. Martin, and P. Rouchon, "Flatness and defect of nonlinear systems: Introductory theory and examples," *Int. J. Control*, vol. 61, no. 6, pp. 1327–1361, Jun. 1995.
[33] K. H. Guo, "Preview following theory and vehicle motion simulation of man-vehicle closed-loop system in large steering angle," *Automobile Eng.*, vol. 14, no. 1, pp. 1–11, 1992.
[34] H. Xiang, "Vehicle control method research for steering stability based on annular region," M.S. thesis, School Transp., Jilin Univ., Changchun, China, 2006.

YUQIONG WANG received the M.S. degree in vehicle operation engineering from Jilin University, Changchun, China, in 2015. She is currently pursuing the Ph.D. degree in mechanical engineering with the School of Transportation and Vehicle Engineering, Shandong University of Technology, Zibo, China. Her research interests include intelligent vehicle dynamics and control, and nonlinear system control.

SHUMING SHI received the B.S. degree in automotive engineering and the Ph.D. degree in vehicle operation engineering from Jilin University, Changchun, China, in 1987 and 1998, respectively.

From 2001 to 2002, he was a Senior Visiting Scholar with TNO Automotive, Netherlands. Since 2004, he has been a Professor with Jilin University and the Academic Leader of the Vehicle Operation Simulation Group, Transportation College. He serves as a part-time Professor of the Wuhan University of Technology. He presided over three projects of the National Natural Science Foundation, four provincial and ministerial projects, and more than ten enterprise projects. He is the author of one textbook of the national 11th five-year plan, more than 40 academic articles, and more than ten inventions. His research interests include nonlinear vehicle dynamics and control, vehicle state estimation, and the driving cycle generation.

Dr. Shi serves as the Vice Chairman of Intelligent Transportation Committee of Chinese Artificial Intelligence Society.

SONG GAO is currently the Dean and a Professor with the School of Transportation and Vehicle Engineering, Shandong University of Technology, Zibo, China. He is also a Middle-Aged Expert with outstanding contribution in Shandong Province and the Executive Director of the China Automotive Engineering Society. He has presided over the national 863 plan of electric vehicle major project and more than 30 other projects. His current research interests include energy system matching theory and the control technology of electric vehicle, intelligent vehicles, and intelligent transportation systems.

Dr. Gao has received the Second Prize of national level teaching achievements and six prizes of provincial level scientific and technological progress.

YI XU received the B.S. degree in transportation from Ludong University, Yantai, China, in 2011, and the Ph.D. degree in vehicle operation engineering from Jilin University, Changchun, China, in 2016. He is currently a Lecturer with the School of Transportation and Vehicle Engineering, Shandong University of Technology, Zibo, China. He has authored over ten academic articles in journals. His research interests include intelligent vehicle environment perception, and dynamic decision and planning.

PENGWEI WANG received the M.S. degree in mechanical design and theory from Jiangxi Agriculture University, Nanchang, China, in 2015. He is currently pursuing the Ph.D. degree in mechanical engineering with the School of Transportation and Vehicle Engineering, Shandong University of Technology, Zibo, China.

His research interests include intelligent vehicle dynamic decision and planning, and intelligent vehicle dynamics and control.